

# Twins: Device-free Object Tracking using Passive Tags

Jinsong Han<sup>\*</sup>, Chen Qian<sup>§</sup>, Xing Wang<sup>\*</sup>, Dan Ma<sup>\*</sup>, Jizhong Zhao<sup>\*</sup>, Pengfeng Zhang<sup>\*</sup>, Wei Xi<sup>\*</sup>, and Zhiping Jiang<sup>\*</sup>

<sup>\*</sup>School of Electronic & Information Engineering, Xi'an Jiaotong University

<sup>§</sup>Department of Computer Science, University of Kentucky

**Abstract**—Device-free based object tracking provides a promising solution for many localization and tracking systems to monitor non-cooperative objects which do not carry any transceiver such as intruders. However, existing device-free solutions mainly use sensors and active RFID tags, which are much more expensive compared to passive tags. In this paper, we propose a novel motion detection and tracking method using passive RFID tags, named *Twins*. The method leverages a phenomenon called critical state caused by interference among passive tags. We theoretically explain this phenomenon via an interference model and conduct extensive experiment to validate it. We design a practical *Twins* based intrusion detection system and implement a real prototype with commercial off-the-shelf reader and tags. Experimental results show that *Twins* is effective in detecting the moving object, with low location errors of 0.75m in average.

**Keywords**—Device-free, Passive RFID tag, Tracking, Critical State

## I. INTRODUCTION

Preventing illegal or unauthorized access of intruders is of importance to protect the security of people, organizations, and their properties. For anti-intrusion purpose, there is an essential need to deploy security systems well-supported by localization and motion-detecting methods. To this end, existing work performs motion detection using various sensors including passive infrared (PIR) sensors, sonic sensors, and video camera sensors. Those methods, though being able to achieve high accuracy and sensitivity, are not cost-efficient for large scale logistic systems, such as retailing, warehouse, cargo transportation, due to various reasons. In recent decades, Radio Frequency Identification (RFID) tags have been widely deployed in modern logistic and inventory systems for efficient identification and monitoring [1-5]. Compared with deploying sensor systems, motion detection using RFID tags for anti-intrusion purpose has two main advantages: low cost and reuse of existing RFID infrastructure.

Motion detection or trajectory tracking by RFID tags has been proposed in the literature [6-12]. There are two major categories in previous work, device-based and device-free methods. By attaching a tag to an item, the device-based method can identify the location of this item when the tag is interrogated by the reader. However, it is impossible to bind tags to uncooperative objects, e.g. the intruders. Thus device-based methods are not suitable for intrusion detection [13] and tracking in many practical applications. Device-free solutions are promising to track intruders while keeping them unaware of detection[14].

However, most existing solutions are based on active tags to achieve device-free object tracking [8, 12, 15]. An active tag is much more expensive than a passive tag, which is too cost-ineffective for large-scale applications. To our knowledge, there is no solution in the literature that can achieve accurate and reliable device-free motion detection with passive RFID tags.

In this paper, we present a novel motion detection and tracking method using passive RFID tags, named *Twins*. Our method is motivated from a phenomenon due to the coupling effect among passive tags. Suppose we put the antennas of two passive tags close and parallel to one another, as illustrated in Fig.1. Within a certain distance, the two adjacent tags will present such a phenomenon that one or both of them, e.g. tag *B* in the left subfigure of Fig.1, just becomes unreadable, due to the coupling effect. As a result, the signal strength of RF waves sent from the reader is significantly reduced at *B*'s antenna. Thus tag *B* cannot receive sufficient energy to perform the computation or modulation, and cannot be read by the reader. We name such a situation as *critical state* and such a pair of tags as *Twins* or a *Twin pair* here after.

Prior work usually attempts to avoid such a phenomenon to improve the successfully reading rate for tags. However, we utilize this phenomenon to achieve device-free motion detection. The key insight is to create a critical state of two tags as *Twins*. If an object or human being moves close to the *Twins*, as shown in the right subfigure of Fig.1, some RF waves will be reflected or refracted to the *Twins*, similar to the multipath effect. In this case, the unreadable tag can receive sufficient energy to break the critical state and then become readable. We call this change as a *state jumping*.

We further design a tracking scheme to achieve accurate trajectory monitoring for moving objects. Our scheme employs a combination of a KNN based algorithm and particle filter based algorithm to approximate the trajectory of intruders. We summarize the major contributions and results of our work as below.

1) We are the first to propose to use critical state of passive tags for intrusion detection and trajectory tracking. By reusing the existing RFID infrastructure, this method is a cost-efficient and accurate anti-intrusion solution.

2) We conduct extensive experiments on a real RFID system for validating the feasibility of using critical state for motion detection.

3) We design a tracking scheme for effective intruder detection and tracking. We have implemented it in a real RFID

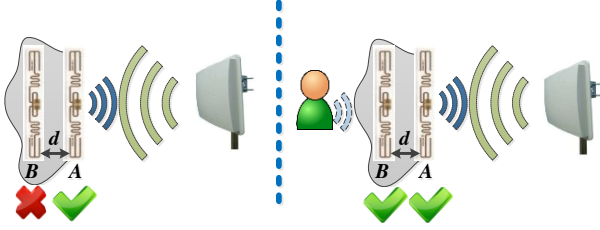


Fig. 1. Critical state of Twins. Left figure shows Tag B cannot be read due to the coupling effect. Right figures show when an object comes, Tag B becomes readable.

system using off-the-shelf reader and tags. The experimental results show that our solution can achieve high detection accuracy, i.e. the localization error is 0.75m in average.

## II. BACKGROUND

As the most representative technology of “untouchable” identification, RFID shows many advantages over the conventional labeling techniques. RFID tags can be automatically and remotely interrogated in a non-line-of-sight way. Current RFID tags fall into two categories, active and passive tags. With on board batteries, active tags have a larger communication region and more powerful computation capacity than passive tags, while suffering from much higher manufacture cost. Passive tags are more cost-efficient. They are battery-free and with simple circuitries.

### A. Near-field and Far-field

In RFID systems, the reader and tags communicate via their antennas. The communication patterns include near-field and far-field communications. The boundary between near-field and far-field is determined by the Rayleigh length [16], calculated as  $R = 2D^2/\lambda$ , where  $D$  is the size of antenna and  $\lambda$  is the wavelength of antenna. Equivalently,  $D$  is the diameter of the smallest sphere enclosing the antenna. Passive tags are identified by using the far-field communication. According to FCC regulation, passive tags should operate in a spectrum of 902~928 MHz in US. With far-field links, RFID reader interrogates the tag by emitting RF waves, while the passive tag modulates its data into the wave reflected to the reader. This pattern is referred as *Backscatter* communication [17]. On the other hand, the interference between two adjacent tags takes effect as a *coupling effect* in the near-field.

### B. Coupling Model of Twins

In the near-field communication, the interaction between two tags’ antennas is known as *inductive coupling* [12]. Theoretically, the antenna of a given tag can be replaced by an equivalent circular loop [18], which is a common and simple equivalent method. Here, the circular loop is not related to the specific structure of tags. Two nearby tags can be modeled by two circular loops as shown in Fig. 2 and in this coordinate system, the center positions of Tag 1 and Tag 2 are  $(0, 0, 0)$  and  $(0, D\sin\phi, D\cos\phi)$ , where  $\vec{D}$  is the vector from center of Tag 1 to the center of Tag 2 and  $\phi$  is the angle between Z axis and  $\vec{D}$ . According to the *Biot-Savart* Law [16] a steady current  $I_1$  at a position  $P$  on the circular of Tag 1 can generate a magnetic field  $B_2$  on Tag 2:

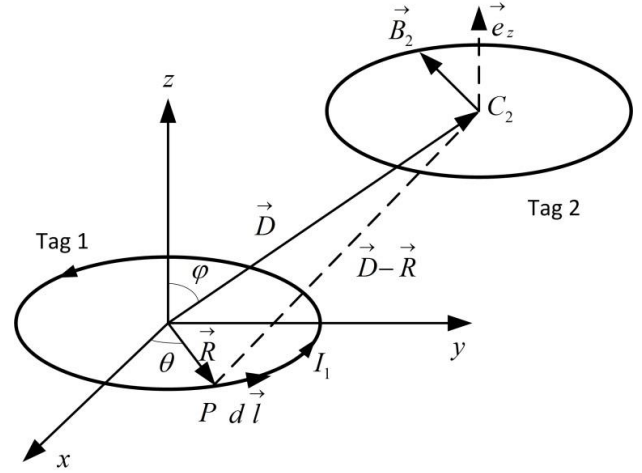


Fig. 2. Model of two coupling tags.

$$B_2 = \frac{\mu_0}{4\pi} \int_0^{2\pi} I_1 d\vec{l} \times \frac{(\vec{D} - \vec{R})}{|\vec{D} - \vec{R}|^3} d\theta \quad (1)$$

where  $\mu_0$  is the magnetic constant,  $d\vec{l}$  is a vector whose magnitude is the length of the differential element of the wire in the direction of conventional current,  $\vec{R}$  is the radius vector along the angle  $\theta$ , and  $\vec{D} - \vec{R}$  is the positional vector starting from the current segment on the Tag 1’s antenna loop and pointing to the center of Tag 2’s loop.

Here we introduce the concept of the *mutual inductance*  $M$ , which is a measure of the coupling between two indicators. Let  $\Psi_{21}(I_1)$  denote the magnetic flux through Tag 2’s loop due to the current in Tag 1. Then the mutual inductance  $M_{21}$  can be written as:

$$M_{21} = \frac{\Psi_{21}(I_1)}{I_1} \quad (2)$$

According to the magnetic flux definition,  $M_{21}$  has the form:

$$M_{21} = \frac{B_2 A_2}{I_1} \quad (3)$$

Here  $A_2$  represents the area of the Tag 2’s loop surface where the magnetic field passing through. Applying Equation (1) to Equation (3), the mutual inductance  $M_{21}$  can be written as:

$$M_{21} = \frac{\mu_0 A_2}{4\pi} \int_0^{2\pi} \frac{d\vec{l} \times (\vec{D} - \vec{R})}{|\vec{D} - \vec{R}|^3} d\theta \quad (4)$$

The induced electromotive force (EMF)  $E_2$  in Tag 2 can be calculated by the *Faraday’s law of induction* [13]. The calculation is based on the fact that the induced EMF in a coil of  $N$  loops is produced by a change in flux in a certain time interval:

$$E_2 = -N \frac{\Delta \Psi_{21}(I_1)}{\Delta t} \quad (5)$$

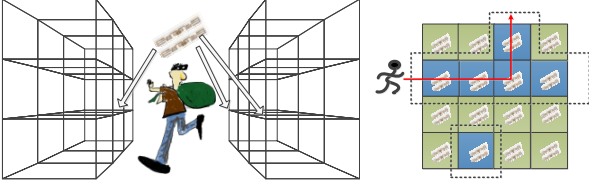


Fig. 3. Intruder detection in a warehouse.

Note  $N$  equals 1 in our model. The negative sign in Equation (5) is derived from the fact that the induced EMF is opposed to any change in the magnetic flux, which is summarized in Lenz's law [16].

As a result, the induced current  $I_{B_2}$  in Tag 2 can be calculated from an equivalent RCL circuit of the tag. Applying Equation (2) and (5), the induced current in Tag 2 is given by:

$$I_{B_2} = \frac{-j\omega M_{21}I_1}{R_2 + 1/j\omega C_2 + j\omega L_2} = -b_2 M_{21}I_1 \quad (6)$$

where  $R_2$ ,  $C_2$ ,  $L_2$  are the chip impedance, capacitance, and inductive impedance of Tag 2, respectively. We let  $b_2$  denote the hardware-relative part of the equation above.

Let  $I_{01}$  and  $I_{02}$  represent the currents of Tag 1 and Tag 2 generated by harvesting the RF signals from the reader, then the current in Tag 2 can be represented as:

$$I_2 = I_{02} + I_{B_2} = I_{02} - b_2 M_{21}I_1 \quad (7)$$

Analogously, the current in Tag 2 can also generate induced current in Tag 1, which means there exists another mutual inductance  $M_{12}$ . As a result, for the current in Tag 1, we can also have:

$$I_2 = I_{01} - b_1 M_{12}I_2 \quad (8)$$

From Equation (7) and (8), we conclude that because of the coupling effect between two tags close to each other, the current induced by the reader's RF waves might be partially offset by a current induced by the coupling effect. Therefore, even both tags of Twins are in the effective range of reader's interrogation, one or both of them will become unreadable. For further validating the feasibility of Twin pair's critical state, we conduct extensive experiments and report the result in Section IV.C.

### III. TRACKING MOVING OBJECTS USING CRITICAL STATE

The tracking procedure comprises of two phases. In the first phase, the state jumping on Twins is identified. In the second phase, we use a particle filter [19] based scheme to track the object. Note that we focus on tracking a single object in this paper and leave multiple-object tracking in future work.

A number of Twins are deployed in the given area, for instance, the alleyway between two shelves with valuable items. We assume each Twins is fully covered by at least one reader's interrogation. The entire region is partitioned into a 2D grid, as shown in Fig.3. In practice, the distance between two pairs of Twins, i.e., the length of cells edges, can be determined based on measurement results. We can formulate the grid as a graph

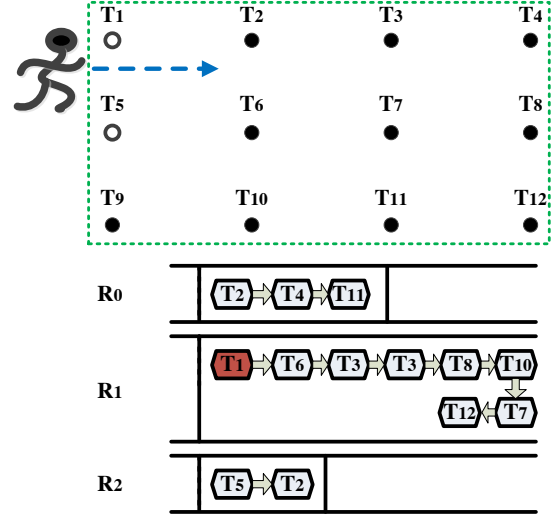


Fig. 4. Example of moving object tracking

$G = \langle V, E \rangle$ , where each cell in the grid is a vertex in  $G$ , and two adjacent cells have an edge in  $G$ . If state jumping is detected at Twin pairs, the corresponding cells will be highlighted as shown in Fig. 3.

#### A. Identifying state jumping

When an object moves in the monitored region, it triggers a serial of state jumping events on multiple Twin pairs. Timely outlining the regions including these Twin pairs is essential to track the object movement. However, there remains a challenging issue. At any time, the reader can only have a fixed value of transmission power  $P_{TX}$ . Therefore the reader can only create the critical state for one Twin pair at a same time. Intuitively, the reader can iteratively and sequentially query all Twin pairs within its detection region. However, sequential queries may miss state jumping, if the movement is so fast that the object has moved out of the cells when the Twin pairs are queried. Using a more sophisticated strategy, the reader can preferentially query the nearby Twin pairs of the Twins that just had state jumping. However, scheduling starvation may occur on some Twin pairs if they have low priority in such scheduling.

To deal with this problem, we propose a simple polling algorithm to achieve timely and efficient movement detection without introducing starvation. Given  $N$  Twin pairs in the system, the objective of the polling algorithm is to find a set  $J$  of Twin pairs with state jumping caused by object movement within a short time interval.

We use the following data structure in our algorithm. For the  $i$ th Twin pair in the graph  $G$ , we store a tuple  $t_i = \langle T, P_{TX}, P, S \rangle$  in the database, where  $T$  denotes the ID number of the Twins,  $P_{TX}$  denotes the corresponding transmission power of reader's antenna to create the critical state for the Twins.  $P$  and  $S$  are two bits representing the query priority and access status of the Twins. If  $P = 1$ , which means the Twins is more likely to have a state jumping, then it has a high priority to be queried. Bit  $S$  indicates whether the Twins has been accessed in a polling round and hence we can avoid unnecessary queries.

The polling algorithm is iteratively conducted through rounds of querying the Twins whose  $P$  is 1. The idea behind our polling algorithm is that if a Twin pair is experiencing a state jumping, its neighboring Twins are most likely to be triggered by the object movement, i.e., having a state jumping. Thus, those Twin pairs should be set with a high priority to be queried. We construct a linked list  $L$  to order such Twins. If this list is empty, the system will randomly choose some Twin pairs and move their neighboring Twin pairs to list  $L$  in the next round. Such a treatment can address the “cold start” problem.

Figure 4 shows an example of our algorithm. At the beginning, we randomly select Twin pairs  $T_2$ ,  $T_4$  and  $T_{11}$  in the polling round  $R_0$ . Before the start of the next round  $R_1$ , we set the bit  $S$  to 0 for all Twin pairs in database. Then, we replace each Twins in  $L$  with their neighboring Twin pairs, e.g. replacing  $T_2$  with  $T_1$ ,  $T_6$ , and  $T_4$ . As a result, in the round  $R_1$ , the Twins in list  $L$  are  $[T_1, T_6, T_3, T_3, T_8, T_{10}, T_7, T_{12}]$  and their priority bit  $P$  are set to 1. During the round  $R_1$ , we sequentially access the tuple of Twins in  $L$ . For each Twin pair in the list, we will check whether its  $S$  is zero. If  $S = 0$ , which means this Twin pair is unvisited, we query this Twins by setting the transmit power of reader to its  $P_{TX}$ . If it is experiencing a state jumping, we will keep it in  $L$ . For any Twins removed from  $L$ , we set its  $P = 0$ . For the example in Fig. 4, suppose that in  $R_1$ , Twins  $T_1$  and  $T_5$  are triggered due to the moving object. Therefore,  $T_1$  will stay in the list while  $T_6$  and  $T_3$  will be removed, while their  $P$  is set as 0. At the end of each query on a pair of Twins, we will set its  $S = 1$  to indicate that this Twins has just been checked in this round. For instance, the second  $T_3$  in  $L$  will be removed from  $L$  when it is checked in  $R_1$ . We check all Twins in  $L$  using above rules in each round. At the end of  $R_1$ , only  $T_1$  is retained and its neighboring pairs  $T_2$ ,  $T_5$  are selected to be moved in  $L$  in the next round.

In short, the algorithm can identify all Twin pairs having state jumping in a short time interval with high probability. These Twin pairs along with the timestamps of the queries will be used for drawing a region where the object most likely stays.

### B. Localizing an object

Based on the detected state jumping on Twins, we can outline the region where the object stays. Ideally, the region should be represented by a connected subgraph  $G_s$  in  $G$ . However, the movement of an object may render several subgraphs unconnected in  $G$ , due to the multi-path effect or ambient noise. We show an example of two separate regions in Fig. 3. In this case, we simply select the largest subgraph in  $G$ , termed as  $G_s$  and filter other disconnected ones out. If there are more than two subgraphs,  $G_s$  is set to the minimum connected component in  $G$  that includes all subgraphs.

After determining the possible region that the object stays, we estimate the current position of the object by calculating the centroid of the positions of all Twins in this region. Suppose there are  $k$  Twin pairs in the region whose positions are  $X_1, X_2, \dots, X_k$ , respectively. The estimated position is  $C = (X_1 + X_2 + \dots + X_k) / k$ . We evaluate the tracking accuracy in Section IV.

### C. Tracking the object based on particle filter

A particle filter is designed to optimize the estimation for non-linear and non-Gaussian state-space models. The main principle of particle filter is to introduce a group of “particles”, which actually are random samples in the state space. Utilizing those particles, the distribution of a latent variable can be “filtered” (approximated) at a specific time, given all observations up to that time. By iteratively filtering and re-sampling, the state of the system or targeted object can be estimated. If the state contains the position or derivatives of the position, we can achieve the trace of the object.

Suppose that an object moves into the monitored area. We set the main entrance of the area as the origin of coordinates. In Fig.5,  $n_0 \sim n_8$  represent the times of state jumping at the corresponding Twins in  $\Delta t$ . We define the vector  $V = (n_0, n_1, n_2, \dots, n_8)$  as the observation.

A particle filter is performed via two phase, offline training and online detecting. In the former phase, we estimate the marginal distribution of  $n_i$  and the position of object  $l$ :

$$P(n_1, n_2, \dots, n_N | l) = \prod_{i=1}^N P(n_i | l)$$

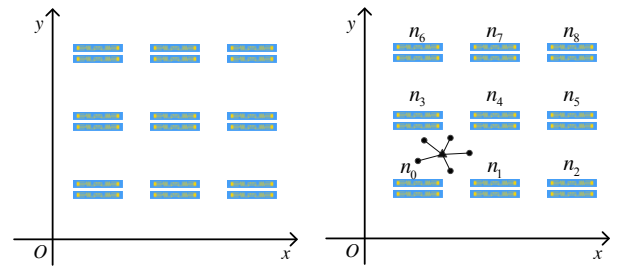
Note that  $l$  is known in the offline training phase. The estimation discretizes the distribution  $P$  into histogram bins, and forms the fingerprint of the position  $l$ .

In the second phase, particle filter is conducted by performing the following steps.

a. Initialization. Suppose the object is located in the origin of coordinates, with a speed as  $v = \langle x_v, y_v \rangle$ , where  $x_v$  and  $y_v$  are the X-component and Y-component of speed  $v$ , respectively.  $N$  particles are sampled near the origin of coordinates.

b. Prediction. The  $p(X_k | Z_{1:k-1})$  is computed from the filtering distribution  $p(X_{k-1} | Z_{1:k-1})$  at time  $k-1$ .

c. Weight computation. The position of each particle is known. Computing the weight depends on two elements, the observation obtained by the measurement as well as the probability distribution of the times of state jumping at each particle's position. The weight is indeed the probability of yielding the observation at each particle.



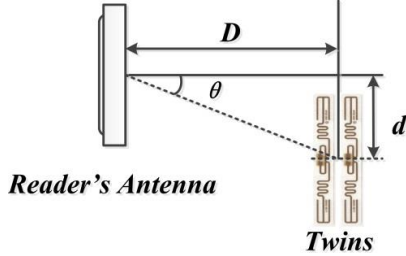
(a) Twins grid (b) An object is in the area

Fig.5. Particle filter.





Fig. 6. Experiment hardware



(a) Calibration experiment



(b) Prototype system

Fig. 7. Experiment setup.

d. Re-sampling. We use the multinomial resampling [20] to remove the particle with low weight with high probability.

e. Approximation. With the position and weight of each particle, we can approximate the coordinates for the object at time  $k$ .

f. Let  $k = k + 1$ , and iteratively perform the steps (b) – (f).

#### IV. IMPLEMENTATION AND EVALUATION

In this section, we describe the prototype implementation and performance evaluation. We conduct the experiments in two aspects. First, we investigate the performance of critical state creation and detection. Second, we implement a Twins prototype and conduct comprehensive experiments to evaluate the effectiveness and efficiency of object tracking.

##### A. Hardware

Figure 6 shows the key hardware components in our prototype. The hardware is entirely built from current commercial products and requires no modification on both the reader and tag sides. The reader is an Impinj Speedway R420, using the EPCglobal UHF Class 1 Gen 2/ISO 18000-6C air protocol. The reader antenna operates in a spectrum of 920 ~ 928MHz. The transmission power ranges from 10 to 32.5



Fig. 8. Validation setup.

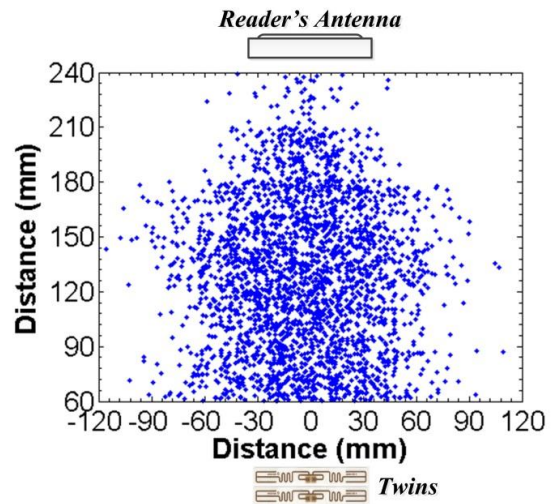


Fig. 9. # of state jumping.

dBm. We use 500 E41-b tags in our experiments. E41-b is a widely-deployed off-the-shelf passive tag from Impinj.

##### B. Methodology

###### 1) Calibration

The goal of calibration is to determine the proper settings of Twins for motion detection. We investigate the performance of a Twin pair in detecting moving objects nearby. As shown in Fig.7 (a), we find proper values for distance  $d$  and angle  $\theta$  between the antennas of Twins and the reader, distance between the Twins and moving object, and height from the Twins to the floor  $h$ .

###### 2) Prototype

In the experiment, we implement our prototype system for the surveillance in a warehouse. We setup a testbed with a number of real shelves aligned as shown in Fig.7 (b). Each Twins is attached to the shelf. The distance between two shelves is 2m and the distance of two adjacent Twin pairs is 0.6m. A volunteer walks among the shelves. We examine the performance of detection rate and probe the proper settings for practical deployment.

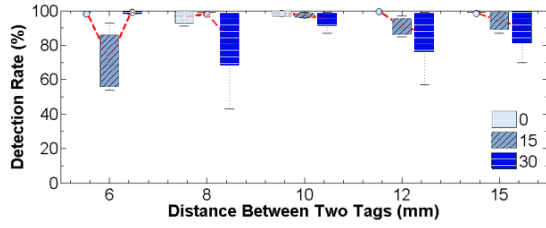


Fig. 10. Calibration result for single Twins.

### 3) Experiment environment

We run the experiments in a large warehouse to evaluate the tracking accuracy of Twins. The area is in a size of 30m×20m and deployed with Twins grid. The height of the intruder is 1.70m and the moving speed is 1.5m/s.

### C. Validation of the Critical State

In this section, we experimentally validate the critical state and state jumping phenomena. First, we deploy two tags A and B as Twins and a reader as shown in Fig.8. We then create a critical state of the Twins by tuning the transmission power of the reader,  $P_{TX}$ . For enabling a fine-grained tuning, we employ a UI of Impinj readers, MultiReader. In this phase, we first set  $P_{TX}$  to 32.5 dBm, and then gradually decrease  $P_{TX}$ . For each step, the reader attempts to interrogate the Twins. A critical state occurs if one or both of them becomes unreadable.

In the next phase, a volunteer moves around the Twins to determine the regions where critical state happens. We record the occurrence of state jumping caused by the moving volunteer and show the corresponding positions in Fig.9. We divide the experiment area into small cells, and count the number of state jumping events in each cell. The results are plotted in Fig.9. This figure geometrically illustrates the sensitivity of detecting the moving object. It can be found that the effective range of detection is relatively large, about a 2m × 1m rectangle between the reader and Twins. When the volunteer moves behind the Twins, the effective range of detection is reduced to 1m away from the Twins.

### D. Performance Evaluation

#### 1) Key parameters of Twins

Through extensive calibration, we investigate the crucial settings in the creation of critical state. We evaluate the impact of different factors on the successful detection rate  $r$  of the moving object in the monitoring region.

The main lobe width of the reader's antenna used in the prototype is 70°. Thus, it is not necessary to set a  $\theta$  larger than 35°. We exam the value of  $r$  by varying  $\theta$  as 0°, 15° and 30°. For each value of  $\theta$ , we vary the distance  $D$  by 75cm, 105cm, 135cm, and 165cm. With each value of  $D$ , we set the distance  $d$  as 6mm, 8mm, 10mm, 12mm, and 15mm. Therefore, we have 3\*4\*5=60 test cases. For each case, we conduct 100 runs of experiments. The result is summarized in Fig.10. The X axis contains different settings of  $d$ . The Y axis represents the detection rate  $r$ . We differentiate the settings of angle with different colors. We have an observation that setting  $d = 10$ mm

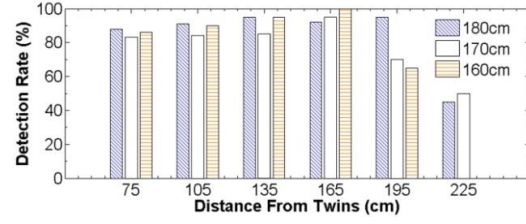


Fig. 11. Impact from the object with different heights

can result in the maximum  $r$  in most cases. We then adopt a default setting of  $d$  as 10mm in the following experiments.

We invite three volunteers to play the role of intruders and walk among the shelves in our prototype. The three volunteers are 160cm, 170cm, and 180cm in height, respectively. Their average walking speed is 1.5m/s. The results are reported in Fig.11. We find that the system has a higher detection rate on taller persons. The reason is that the taller person has a larger cross-sectional area such that more RF waves can be reflected to the Twins, yielding a state jumping with higher probability. We also notice that the detection rate is always over 80% for all volunteers, and 90% for the volunteers with a 1.70m+ height. This result shows that our system is relatively height-insensitive in detecting human movements.

Our system is also feasible when changing the distance between Twins and reader antenna  $D$ . We vary the value of  $D$  and exam the transmission power  $P_{TX}$  to drive the Twins into the critical state. According to Fig.12, we find that a larger  $D$  requires a higher  $P_{TX}$ . Therefore, the maximum deployment distance of Twins depends on the maximum transmission power of reader, e.g. 5.8m when  $P_{TX} = 32.5$ dbm if using the Impinj R420 reader.

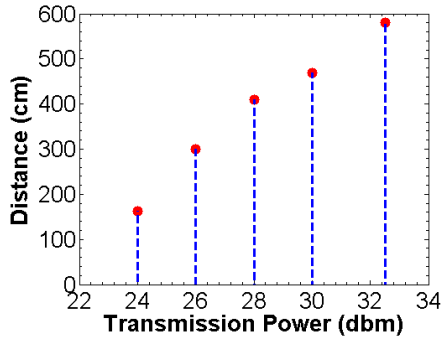
#### 2) Tracking accuracy

We investigate the accuracy of Twins-based tracking scheme and compare it with two well-known RFID based device-free approaches, LANDMARC [8] and TASA [12] through experiments. LANDMARC is active tag based and TASA is a hybrid systems of active and passive tags. The tags are deployed in a tag array in all three approaches. The distance between the nearest neighbors in a row or column is 1m for LANDMARC and 0.6m for TASA. During the procedure of tracking the simulated intruder, we use the distance from the estimated position to the real position as the localization error for each experiment. The results plotted in Fig.13 exhibit that the Twins method has a better tracking accuracy than both of LANDMARC and TASA in average. Although Twins is not accurate in a small portion of positions on the moving path, its position error rate is always below 0.85m, which is 0.75m in average.

## V. DISCUSSION

### A. Proper detection region

Observed from our experiments, state jumping is much easier to occur if the object sits between the Twins and the reader, instead of being behind the Twins. It is mainly because

Fig. 12.  $P_{TX}$  vs.  $D$ .

the object moving behind triggers a weaker disturbance to the RF signals around the Twins than in the “in-between” space. Furthermore, detection becomes much unreliable if the Twins are attached to items. In our implementation and experiments, we adopt the “in-between” deployment for the reader and Twins.

### B. Critical state of a single tag

Instead of using two adjacent tags, we can use a single tag for the moving detection via its own critical state. That is, the reader can probe using the minimum transmission power that can identify a tag in a given position. If one object moves nearby, the tag may also become readable. We perform the experiment on single tag and find that the single tag is, however, more unstable than Twins in controlling critical states. The reason is that a single tag is more susceptible to the ambient changes. While this may lead more sensitivity to the single tag, the stability, i.e.,  $P_{TX}$  required at the reader for generating critical state varies much drastically than Twins. We leave the study of addressing the stability of critical state for a single tag in our future work.

### C. Multiple moving objects

In this work, we focus on tracking of single object. If the area monitored has multiple moving objects, can we still be able to detect them using the Twins method? Indeed, the Twins based tracking scheme has a potential solution. Actually, if there are multiple objects moving in the area, their movements may result multiple subgraphs in  $G$ . Intuitively, we can track those objects via those subgraphs. However, there are many challenges in plotting the subsequential traces for those objects, considering the scenario that their moving trajectories may cross or overlap. Since tracking multiple objects is out of the scope of this paper, we will give a solution in our future work.

## VI. RELATED WORKS

The idea of utilizing wireless signals for activity sensing is not new [8, 21, 22]. It continuously attracts attentions recently, due to the prevalence of today’s wireless and mobile devices. Research community has proposed many proposals for localizing and tracking objects by using rich sensors and various context attributes, including the GSM [23], WiFi [24], GPS [25], FM [26], acoustic [27] and optic [28] signals. Prior works in the literature can be categorized into two groups, device-based and device-free approaches. The former pattern

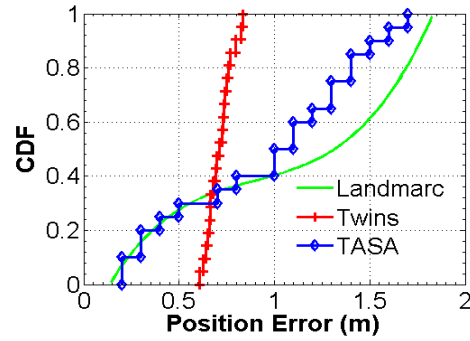


Fig. 13. Tracking accuracy.

normally requires a device to be bound with the target, while the latter one has no need to bind a device to the target.

Device-based approaches require the target attaching or holding a transceiver. Among those works, LANDMARC [8] is a pioneering work of exploiting the RSS change for localization and tracking. It first site-surveys the RSS-based position fingerprint of a tag-array-covered area. Tracking an active tag can be realized by matching the collected RSS change with the position fingerprint [8] [15]. There is a growing interest in crowdsourcing the sensing capacity of a large amount of computing devices that are held by unprofessional users, such as the works Zee [29] and LiFS [30].

Passive tag based localization is often deployed in the warehouse or library for accurately locating the desired item or book [9, 31, 32]. Choi et al [32] propose a localization algorithm LDTI. LDTI locates the box in a shelf by detecting the tag-interference among the reference tags and target tag. PinIt [31] is one of the most recent works that exploit a passive tag’s multipath profile for positioning the object. The work employs the synthetic aperture radar (SAR) imaging mechanism to achieve high accuracy in locating the passive tag. The work shows a promising direction for leveraging multipath effect for localizing low-cost mobile devices.

However, the device-based works requires the desired object to be with a device for localization, which are orthogonal to Twins.

On the other hand, Device-free Passive (DfP) localization is more suitable for monitoring uncooperative objects. Most prior works leverage the disturbance to the wireless signals for monitoring the intruding object. Youssef et al. demonstrate the DfP feasibility and raise the essential challenges in it [33]. Xu et al. propose an active node based method to use the disturbance from the human body to the RF pattern for indoor localization [34]. A following work SCPL is proposed to model the human trajectory through Viterbi algorithm [11]. Compared to our work, these two works use much powerful active tags and unlicensed RF bands. Meanwhile, the location accuracy of SCPL is 1.3m, lower than Twins based tracking scheme. Although the work [35] has an accurate detection rate, the system utilize active tags, which may introduce a high cost in large scale applications. TASA [12] provides the function of tag-free activity sensing or route tracking. TASA also exploits the RSS change for motion detection. TASA, however, still

need to involve active tags for reliable sensitivity in activity sensing. Differing from these previous device-free works, Twins is solely based on passive tags, which is more cost-effective. Meanwhile, Twins is a novel detecting method that first leverages the critical state phenomenon of coupling tags.

It has been observed that nearby tags can produce interference to each other. Weigand and Dobkin conduct experiments over two tag arrays at two planes [36]. The result reported in [36] shows that the successful interrogation rate of tags is severely affected when two parallel arrays are approaching to each other. Later, Chen et al. propose a model for nearby tags to formulate their interference affect [18].

## VII. CONCLUSION

In this paper, we propose a novel device-free object tracking scheme, Twins. We contribute to both the theory and practice of a new observed phenomenon, i.e., critical state on two adjacent tags. We also design a practical tracking method using passive tags. The extensive real experiments demonstrate the effectiveness of our method. Our future work includes studying critical state on a single tag, utilizing Twins to track multiple objects, and extending the detection region by refining the tracking algorithms.

## VIII. ACKNOWLEDGEMENT

This work is partially supported by the National Natural Science Foundation of China (NSFC) under Grant No. 61190112 and 61373175, and the Fundamental Research Funds for the Central Universities of China under Project No. 2012jdgz02 (Xi'an Jiaotong University). Chen Qian is supported by University of Kentucky faculty startup funding.

## REFERENCES

- [1] M. Shahzad and A. X. Liu, "Fast and Accurate Estimation of RFID Tags," *IEEE/ACM Transactions on Networking*, in press, 2013.
- [2] C. Qian, Y. Liu, H. Ngan, and L. M. Ni, "ASAP: Scalable Identification and Counting for Contactless RFID Systems," in Proceedings of IEEE ICDCS, 2010.
- [3] C. Qian, H. Ngan, Y. Liu, and L. M. Ni, "Cardinality Estimation for Large-scale RFID Systems," in Proceedings of IEEE PerCom, 2008.
- [4] L. Yang, J. Han, Y. Qi, and Y. Liu, "Identification-Free Batch Authentication for RFID Tags," in Proceedings of IEEE ICNP, 2010.
- [5] L. Yang, J. Han, Y. Qi, C. Wang, T. Gu, and Y. Liu, "Season: Shelving Interference and Joint Identification in Large-scale RFID Systems," in Proceedings of IEEE INFOCOM, 2011.
- [6] X. Zhu, Q. Li, and G. Chen, "APT: Accurate Outdoor Pedestrian Tracking with Smartphones," in Proceedings of IEEE INFOCOM, 2013.
- [7] S. Guha, K. Plarre, D. Lissner, S. Mitra, and B. Krishna, "AutoWitness: Locating and Tracking Stolen Property While Tolerating GPS and Radio Outages," in Proceedings of ACM SenSys, 2010.
- [8] L. M. Ni, Y. Liu, Y. C. Lau, and A. Patil, "LANDMARC: Indoor Location Sensing Using Active RFID," *ACM Wireless Networks*, (WINET), vol. 10, iss. 6, pp. 701-710, 2004.
- [9] J. Wang, F. Adib, R. Knepper, D. Katabi, and D. Rus, "RF-Compass: Robot Object Manipulation using RFIDs," in Proceedings of ACM MobiCom, 2013.
- [10] J. Manesilp, C. Wang, H. Wu, and N.-F. Tzeng, "RFID Support for Accurate 3D Localization," *IEEE Transactions on Computers*, vol. 62, iss. 7, pp. 1447-1459, 2013.
- [11] C. Xu, B. Firner, R. S. Moore, Y. Zhang, W. Trappe, R. Howard, F. Zhang, and N. An, "Scpl: Indoor Device-free Multi-subject Counting and Localization using Radio Signal Strength," in Proceedings of ACM IPSN, 2013.
- [12] D. Zhang, J. Zhou, M. Guo, J. Cao, and T. Li, "TASA: Tag-Free Activity Sensing Using RFID Tag Arrays," *IEEE Transactions on Parallel and Distributed Systems (TPDS)*, vol. 22, iss. 4, pp. 558-570, 2011.
- [13] J. Li, J. Chen, and T. H. Lai, "Energy-efficient Intrusion Detection with a Barrier of Probabilistic Sensors," in Proceedings of INFOCOM, 2012.
- [14] Y. Liu, Y. Zhao, L. Chen, J. Pei, and J. Han, "Mining Frequent Trajectory Patterns for Activity Monitoring Using Radio Frequency Tag Arrays," *IEEE Transactions on Parallel and Distributed Systems (TPDS)*, vol. 23, iss. 11, pp. 2138-2149, 2012.
- [15] Y. Zhao, Y. Liu, and L. M. Ni, "VIRE: Active RFID-based Localization Using Virtual Reference Elimination," in Proceedings of 34th International Conference on Parallel Processing (ICPP), 2007.
- [16] R. K. Wangsness, *Electromagnetic Fields*: Wiley-VCH, 1986.
- [17] D. M. Dobkin, *The RF in RFID, Passive UHF RFID in Practice*: Elsevier Inc., 2007.
- [18] X. Chen, F. Lu, and T. T. Ye, "The 'Weak Spots' in Stacked UHF RFID Tags in NFC Applications," in Proceedings of IEEE RFID, 2010.
- [19] A. Doucet, N. D. Freitas, and N. J. Gordon, *Sequential Monte Carlo Methods in Practice*: Springer, 2001.
- [20] M. K. Pitt and N. Shephard, "Filtering via Simulation: Auxiliary Particle Filters," *Journal of the American Statistical Association*, vol. 94, iss. 446, pp. 590-599, 1999.
- [21] Z. Yang and Y. Liu, "Understanding Node Localizability of Wireless Ad Hoc and Sensor Networks," *IEEE Transactions on Mobile Computing*, vol. 11, iss. 8, pp. 1249-1260, 2012.
- [22] D. Ma, C. Qian, W. Li, J. Han, and J. Zhao, "GenePrint: Generic and Accurate Physical-Layer Identification for UHF RFID Tags," in Proceedings of IEEE ICNP, 2013.
- [23] P. Mohan, V. N. Padmanabhan, and R. Ramjee, "Nericell: Rich Monitoring of Road and Traffic Conditions using Mobile Smartphones," in Proceedings of ACM Sensys, 2008.
- [24] K. Wu, J. Xiao, Y. Yi, D. Chen, X. Luo, and L. M. Ni, "CSI-Based Indoor Localization," *IEEE Transactions on Parallel and Distributed Systems (TPDS)*, vol. 24, iss. 7, pp. 1300-1309, 2013.
- [25] J. Liu, B. Priyantha, T. Hart, H. S. Ramos, A. A. F. Loureiro, and Q. Wang, "Energy Efficient GPS Sensing with Cloud Offloading," in Proceedings of ACM Sensys, 2012.
- [26] Y. Chen, D. Lymberopoulos, J. Liu, and B. Priyantha, "Fm-based Indoor Localization," in Proceedings of ACM Mobisys, 2012.
- [27] R. Nandakumar, K. Chintalapudi, and V. Padmanabhan, "Centaur: Locating Devices in an Office Environment," in Proceedings of ACM MobiCom, 2012.
- [28] Y. He, Y. Liu, X. Shen, L. Mo, and G. Dai, "Noninteractive Localization of Wireless Camera Sensors with Mobile Beacon," *IEEE Transactions on Mobile Computing*, vol. 12, iss. 2, pp. 333-345, 2013.
- [29] A. Rai, K. K. Chintalapudi, V. N. Padmanabhan, and R. Sen, "Zee: Zero-Effort Crowdsourcing for Indoor Localization," in Proceedings of ACM MobiCom, 2012.
- [30] Z. Yang, C. Wu, and Y. Liu, "Locating in Fingerprint Space: Wireless Indoor Localization with Little Human Intervention," in Proceedings of ACM MobiCom, 2012.
- [31] J. Wang and D. Katabi, "Dude, Where's My Card? RFID Positioning That Works with Multipath and Non-Line of Sight," in Proceedings of ACM Sigcomm, 2013.
- [32] J. S. Choi, H. Lee, D. W. Engels, and R. Elmasri, "Passive UHF RFID-Based Localization Using Detection of Tag Interference on Smart Shelf," *IEEE Transactions on Systems, Man, and Cybernetics—PART C: APPLICATIONS AND REVIEWS*, vol. 42, iss. 2, pp. 268-274, 2012.
- [33] M. Youssef, M. Mah, and A. Agrawal, "Challenges: Device-free Passive Localization for Wireless Environments," in Proceedings of ACM MobiCom, 2007.
- [34] C. Xu, B. Firner, Y. Zhang, R. Howard, J. Li, and X. Lin, "Improving RF-Based Device-Free Passive Localization In Cluttered Indoor Environments Through Probabilistic Classification Methods," in Proceedings of ACM/IEEE IPSN, 2012.
- [35] Y. Liu, L. Chen, J. Pei, Q. Chen, and Y. Zhao, "Mining Frequent Trajectory Patterns for Activity Monitoring Using Radio Frequency Tag Arrays," in Proceedings of IEEE PerCom, 2007.
- [36] S. M. Weigand and D. M. Dobkin, "Multiple RFID Tag Plane Array Effects," in Proceedings of IEEE Antennas and Propagation Society International Symposium, 2006.